Electronic Supplementary Material (ESI) for Nanoscale.

Supporting Information

Imaging and Analysis of Covalent Organic Framework Crystallites on a Carbon Surface: Nanocrystalline Scaly COF/Nanotube Hybrid

Benjamin L. Weare,[a] Rhys W. Lodge,[a] Nikolai Zyk,[a] Andreas Weilhard,[a] Claire L. Housley,[a] Karol Strutyński,[b] Manuel Melle-Franco,[b] Aurelio Mateo-Alonso,[c,d] and Andrei N. Khlobystov[a]

[a] *School of Chemistry, University of Nottingham, University Park, Nottingham NG7 2RD, UK.*

[b] *CICECO - Aveiro Institute of Materials, Department of Chemistry, University of Aveiro, 3810-193 Aveiro, Portugal.*

[c] *POLYMAT, University of the Basque Country UPV/EHU, Avenida de Tolosa 72, E-20018 Donostia-San Sebastian, Spain.*

[d] *Ikerbasque, Basque Foundation for Science, Bilbao, Spain.*

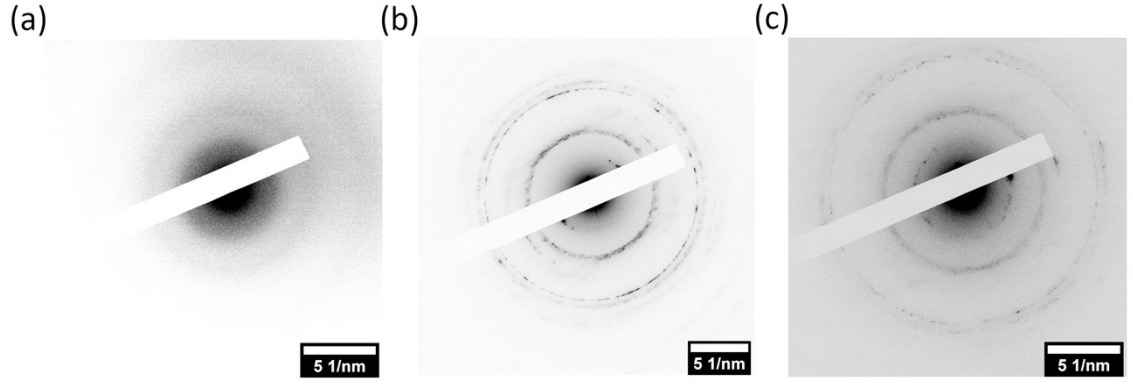

Figure S1: SAED patterns of (a) COF, (b) GNF and (c) COF-GNF hybrid. The lookup tables have been inverted and the contrast adjusted to aid the reader. Very faint diffuse diffraction rings can be observed in the COF and COF-GNF hybrid SAEDP.

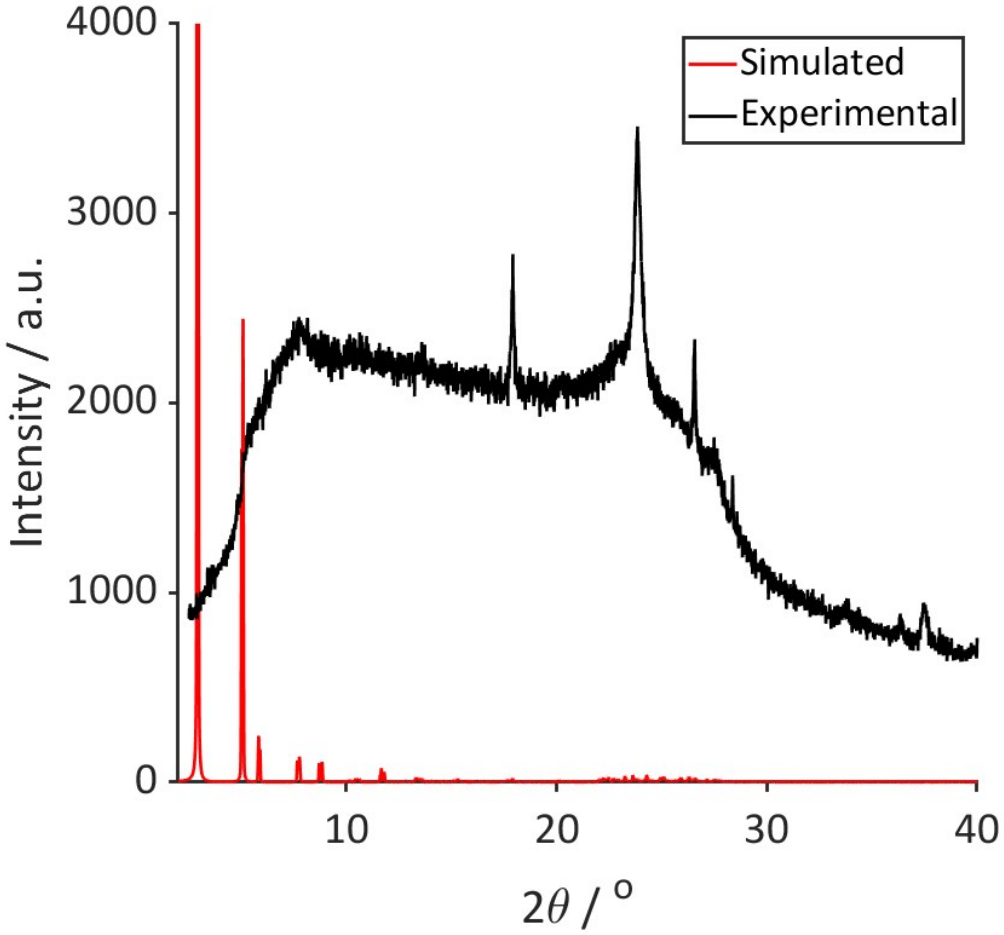

Figure S2: Experimental PXRD diffractogram of COF (black), with peaks at 17.9 °, 23.8 °, 26.5 °, and 28.4 °. The experimental pattern has a large background signal characteristic of diffuse reflection from amorphous material and broad peaks indicating small crystallites. Simulated PXRD pattern (red) from the modelled COF unit cell (Figure 1b), predicted using Cu($K_{\alpha 1}$) radiation in VESTA (ver 3.5.1).[1] The simulated pattern is typical for a COF material and contains several reflections between 2 °, and 10 ° due to the presence of ordered pores.

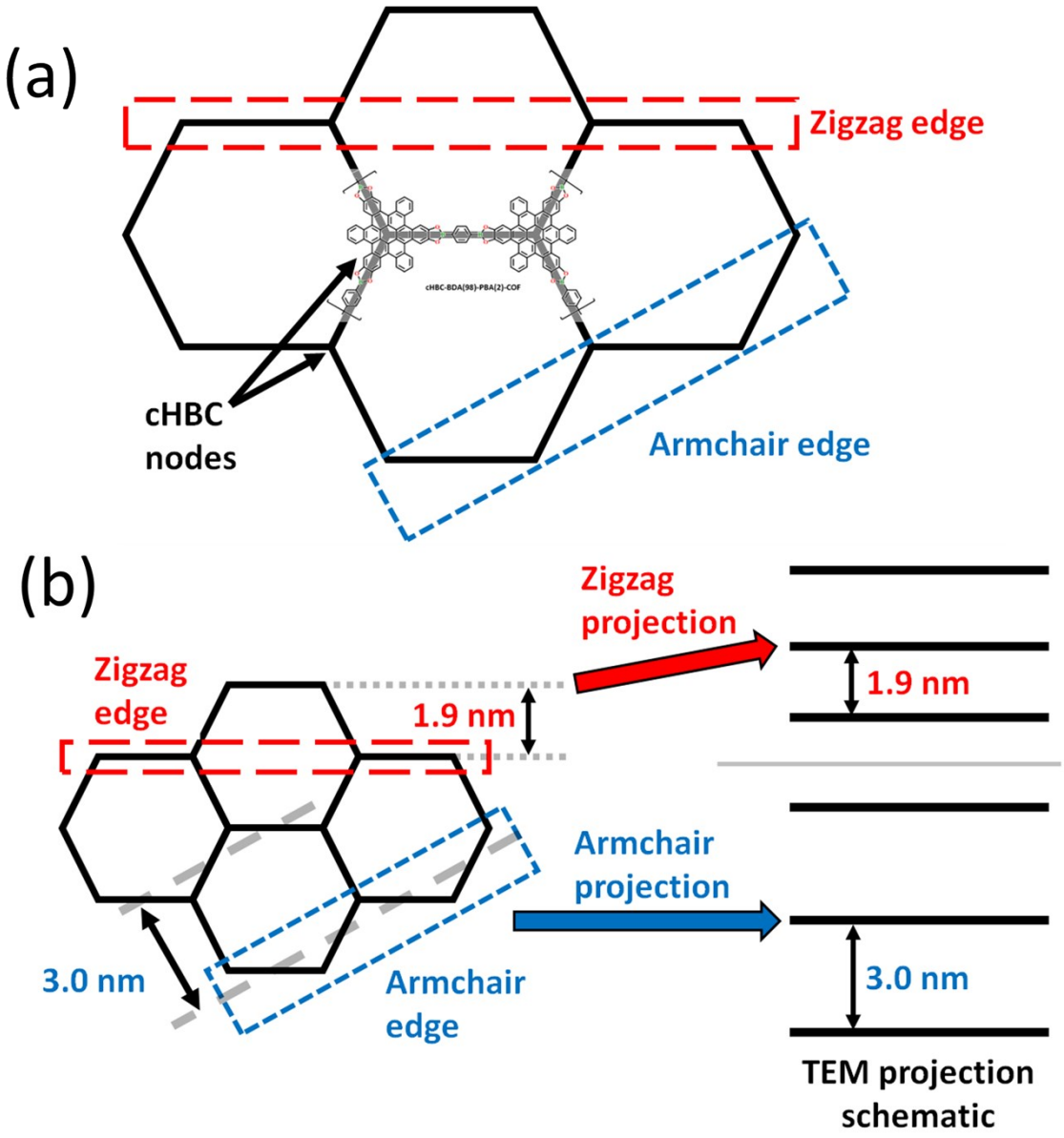

Figure S3: (a) Illustration of zigzag (red box) and armchair (blue box) projections on a hexagonal lattice. For cHBC-BDA(98)-PBA(2) COF the hexagon vertices are occupied by cHBC nodes and the edges by BDA linkers. (b) Illustration of the zigzag (red box) and armchair (blue box) projections and the fringe d-spacing they correspond to.

Wavenumber / cm^{-1}	Vibrational Mode
3402	O-H stretch
1393	Ring breathing (ester)
1333	Ring breathing (ester)/ B-C stretch (acid)
1235	C-O stretch
1079	B-O symmetric stretch (ester)
660	B-O out-of-plane displacement (ester)
601	B out-of-plane bend (acid)
541	OH out-of-plane bend (acid)

Table S1: Assignments for IR spectrum of COF (Figure 1). The boron-containing functional group giving rise to the vibration (boronate ester or boronic acid) is indicated in brackets.

m/z	Assignments
1487	$C_{102}H_{37}B_3O_{12}^+$
1149	$C_{81}H_{26}B_2O_8^+$
1121	$C_{81}H_{30}B_2O_6^+$
1092	$C_{76}H_{29}B_2O_8^+$
882	$C_{59}H_{24}B_2O_8^+$
864	$C_{60}H_{26}B_2O_6^+$
850	$C_{59}H_{24}B_2O_6^+$
826	$C_{55}H_{21}B_3O_7^+$
810	$C_{54}H_{22}B_4O_6^+$
798	$C_{54}H_{21}B_3O_6^+$
782	$C_{54}H_{22}B_3O_5^+$
775	$C_{54}H_{24}B_2O_5^+$
734	$C_{52}H_{19}BO_5^+$
722	$C_{48}H_{18}B_3O_6^+$
712	$C_{48}H_{18}B_2O_6^+$
710	$C_{48}H_{16}B_2O_6^+$
696	$C_{48}H_{24}O_6^+$
694	$C_{48}H_{22}O_6^+$
678	$C_{48}H_{22}O_5^+$
667	$C_{49}H_{20}BO_3^+$
655	$C_{48}H_{15}O_4^+$
649	$C_{46}H_{22}BO_4^+$
638	$C_{46}H_{22}O_4^+$

Table S2: m/z values and formula of key ions in the MALDI-ToF spectrum. All ions in the spectrum were found to be singly charged.

Sample	Distance / nm^{-1}	Reciprocal distance / nm^{-1}	2θ / °
GNF	6.65	0.30	29
	10.92	0.18	49
	13.3	0.14	62
	18.4	0.10	90
	19.8	0.10	99
COF	6.98	0.29	31
	11.78	0.17	54
	18.1	0.11	89
COF-GNF hybrid	6.38	0.31	28
	11.2	0.18	50
	18.6	0.11	91

Table S3: SAED measurements for GNF, COF, and COF-GNF hybrid. The reciprocal of half the diameter of the diffraction rings is used to calculated real space distance, which is then converted to an angle using the Bragg equation. The diffuse rings seen in the COF and COF-GNF hybrid do not correspond to any of the observed COF d-spacings (Figure 3 in manuscript file), but do seem to match with the SAEDP of the GNF, suggesting they are caused by graphitic carbon. The 2Theta values do not match with any peaks in the PXRD pattern. This suggests that diffuse diffraction rings are caused by the amorphous carbon of the TEM grid.

	COF	**COF/GNF hybrid**
Largest parallel measurement / nm	52.5	20.7
Largest perpendicular measurement / nm	59.9	33.1
Most frequent parallel measurement range / nm	14 - 16	10 - 12
Most frequent perpendicular measurement range / nm	20 - 24	18 - 20
Mean parallel measurement / nm	18 ± 16	13 ± 8.0
Mean perpendicular measurement / nm	28 ± 20	22 ± 16
Mean d-spacing and standard distribution / nm	2.8 ± 1.1	2.9 ± 1.1
Mean pore channel angle and standard distribution / °	N/A	75 ± 24

Table S4: Summary of measurements quoted in the text for COF and COF/GNF hybrid. Standard deviations are calculated using Equation S2 and are quoted to 2σ.

Binding fragment	Binding substrate	Binding Energy / eV
Benzenediboronic acid (BDA)	Graphene	-0.781
cHBC	Graphene	-2.139
cHBC-BDA-cHBC	Graphene	-2.219
cHBC-BDA-cHBC (planar)	Graphene	-4.935
COF	Graphene	-2.202
COF (planar)	Graphene	-51142
COF AA bilayer	-	-5.221
cHBC	cHBC	-2.074

Table S5: Binding energies for adsorption of benzenediboronic acid, cHBC, cHBC-BDA-cHBC fragments and COF unit cells onto graphene. Also included are a hypothetical planar cHBC-BDA-cHBC fragment and planar COF, and the binding energies of a COF AA bilayer and cHBC adsorbed onto cHBC.

$$\tau = \frac{K\lambda}{\beta cos(\theta)}$$

Equation S1: Scherrer equation; showing the relationship between crystallite size (τ), Bragg angle (θ), X-ray wavelength (λ), line broadening (β) and shape factor (*K*).

$$\sigma = \sqrt{\frac{\sum (x - \bar{x})^2}{N - 1}}$$

Equation S2: Sample standard deviation (σ), equal to the square root of sum of the squares of the difference between measurement (x) and mean ($\bar{x}$) divided by the number of measurements (N) minus one.

$$n\lambda = 2dsin(\theta)$$

Equation S3: Bragg equation; showing the relationship between wavelength (λ), interlayer distance (d) and Bragg angle (θ).

References

1. K. Momma and F. Izumi, *J. Appl. Crystallogr.*, 2011, **44**, 1272-1276.